Anal. Bioanal. Electrochem., Vol. 11, No. 3, 2019, 416-426

Analytical & Bioanalytical Electrochemistry

2019 by CEE
www.abechem.com

Full Paper

Ethylenediaminetetraacetic Acid and Polyvinyl Chloride Grafted Zinc Cations doped Magnetite Nanoparticles for Biomedical Applications: Electrochemical Synthesis and Characterization

Saeed Kakaei*

Materials and Nuclear Research School, Nuclear Science and Technology Research Institute (NSTRI), P.O. Box 14395-834, Tehran, Iran

*Corresponding Author,
E-Mail: skakaei@aeoi.org.ir

Received: 10 October 2018 / Received in revised form: 23 February 2019 / Accepted: 27 February 2019 / Published online: 31 March 2019

Abstract- In this paper, two-types of superparamagnetic metal-ions doped iron oxide nanoparticles including ethylenediaminetetraacetic acid-grafted Zn^{2+} doped SPIONs (EDTA-Zn-SPIONs) and polyvinyl chloride-grafted Zn^{2+} doped SPIONs (PVC-Zn-SPIONs) nanoparticles are reported. These nanoparticles are fabricated through base generation cathodic electrodeposition method. The surface coat onto the prepared particles and zinc-doping into iron oxide were proved though Fourier-transform infrared spectroscopy, Field-emission scanning electron microscopy and Energy Dispersive X-ray analyses. The magnetic data was provided by sample vibrating magnetometer (VSM) technique. The EDTA-Zn-SPIONs exhibited magnetic performances of *Ms*=34.12 emu/g, *Hci*= 9.1G, *Mr*=0.29 emu/g, $Mr_{(+)}$=+0.21 emu/g, $Mr_{(-)}$=-0.38 emu/g $Hci_{(+)}$=11.28G and $Hci_{(-)}$=-6.75 G. Also, PVC-Zn-SPIONs showed *Ms*=28.45 emu/g, *Hci*=5.75G, *Mr*=0.14 emu/g, $Mr_{(+)}$=-0.11 emu/g, $Mr_{(-)}$=-0.18 emu/g, $Hci_{(+)}$=7.75G and $Hci_{(-)}$=3.75G. These data confirmed the quality of both prepared particles for biomedical applications.

Keywords- Nanoparticles, Electrochemical synthesis, Iron oxide, Doping, Surface grafting

1. INTRODUCTION

In the last decade, many efforts have been paid to design and development of new nanomaterials/nanocomposites for biological, medicinal, environmental, energy storage uses, and also introducing their novel/improved fabrication routes [1-9]. For instance, polymer-magnetite nanocomposites i.e. polymer-grafted superparamagnetic iron oxide nanoparticles (SPIONs) have received more attention due to their various ranges of unique properties, where they are capable to display novel attractive performances in various fields [10-12]. Such magnetic nano-matrixes have found promising applications for uses in various biomedical and environmental applications including magnetic resonance imaging (MRI), cell tracking, drug-delivery systems, imaging, bio-sensing, medical diagnostics, magnetic separation, contaminant removal, remediation, and water treatment [13-18]. In this regard, the surface-grafted SPIONs with various polymers of poly(vinyl alcohol), poly(vinylpyridine), polyethylene glycol, polyethylenimine, chitosan, etc. have been prepared through chemical/electrochemical methods, and their magnetic and physicochemical properties have been examined [19-27]. Ethylenediaminetetraacetic acid (EDTA) is a famous linker for its strong M^{n+}-complexing ability [28,29], which provide excellent metal-binding connection with the adsorbents through surface grafting. EDTA forms the stable connection with surface of SPIONs and hence EDTA-capped-SPIONs as adsorbent have extensively studied [30-36].

As an electrochemical procedure, reductive cathodic electrodeposition has developed as simple and powder tool for obtaining metal oxides/hydroxides nanostructures [37-48]. Hence, reductive electrodeposition can be used to fabrication of surface-grafted SPIONs with biocompatible polymers and EDTA, where the surface-capped nanoparticles are promising candidates for further functionalization and using in various biomedical aims [49-52]. Furthermore, this electrochemical strategy has been studied in the preparation of Fe_3O_4 nanoparticles doped with metal-cations and an improvement in magnetization and remanent of iron oxide has been reported [53-60]. In this work, a simple and one-step reductive deposition is reported for the fabricating ethylenediaminetetraacetic acid-grafted Zn^{2+} doped SPIONs (EDTA-Zn-SPIONs) and polyvinyl chloride-grafted Zn^{2+} doped SPIONs (PVC-Zn-SPIONs) nano-particles. The obtained SPIONs are also characterized through FT-IR, VSM, FE-SEM, XRD and EDAX techniques.

2. EXPERIMENTAL PROCEDURE

2.1. Preparation of SPIONs

The following chemicals used in the synthesis experiments; (*i*) $Fe(NO_3)_3.6H_2O$ (Sigma-Aldrich, 99.99%), (*ii*) $FeCl_2.4H_2O$ (Sigma-Aldrich, 99.5%), (*iii*) $ZnCl_2.4H_2O$ (Sigma-Aldrich, 99%), (*iv*) polyvinyl chloride (PVC, Sigma-Aldrich, average Mw~233,000) and (*v*) ethylenediaminetetraacetic acid disodium salt dehydrate (EDTA-Na_2, Sigma-Aldrich,

99.9%). The electrochemical set-up was two-electrodes of steel 316L cathode and anode with sizes of 5cm*5cm. An aqueous solution of 2g $Fe(NO_3)_3$, 1g $FeCl_2$, 0.5g $ZnCl_2$, 0.5g PVC (in the case of PVC-Zn-SPIONs deposition), 0.5g EDTA(in the case of EDTA-Zn-SPIONs deposition) was used as the electrolyte deposition bath. For electrosynthesis of both samples, the constant current of 15mA/cm^2 was applied for 15min at RT conditions. After deposition, the deposits were separated from the electrode surfaces and used in the further analyses.

2.2. Characterization techniques

The powder X-ray diffraction (XRD) analyses were carried out using a Phillips PW-1800 X-ray diffractometer instrument with a Cu Kα radiation source (λ = 0.154056 nm), and XRD pattern of samples were recorded. The IR spectra were recorded by Bruker Vector 22 IR spectrometer in the wave numbers of 4000–400 cm^{-1}. Field-emission Scanning Electron Microscope (FE-SEM, model Mira 3-XMU with accelerating voltage of 100 kV), attached with Energy Dispersive X-ray Spectroscopy (EDAX) were used to provide morphology observations (FE-SEM images) and elemental composition of samples, respectively. The values of saturation magnetization, remanent and coercivity of sample and its hysteresis profile were measured at room temperature through vibrating sample magnetometer instrument (VSM, Lake Shore 7307).

3. RESULTS AND DISCUSSION

3.1. Crystal structure

The x-ray powder diffraction patterns of the electro-deposited EDTA-Zn-SPIONs and PVC-Zn-SPIONs samples are given in Fig. 1. In both patterns, there are seven diffractions located at 18.21º, 31.75º, 35.68º, 43.52º, 54.71º, 57.05º and 62.36º, which can be assigned to the crystal plans of magnetite (Fe_3O_4) phase of iron oxide, i.e. (111), (220), (311), (400), (422), (511) and (440), respectively.

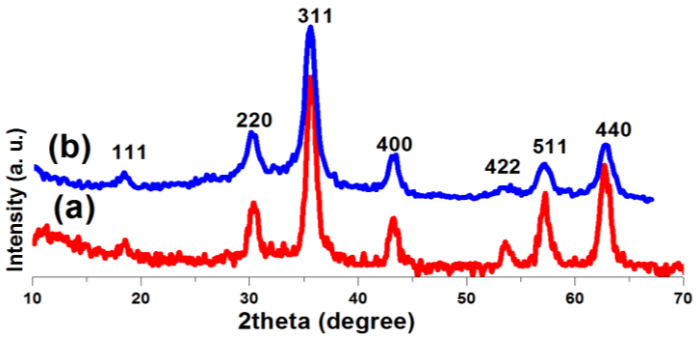

Fig. 1. XRD patterns of the prepared (a) PVC-Zn-SPIONs and (b) EDTA-Zn-SPIONs samples

Hence, magnetite structure is the main phase of both prepared EDTA-Zn-SPIONs and PVC-Zn-SPIONs samples. Furthermore, theses pattern are very similar to those reported for IONPs fabricated by electrochemical routs [58-61]. In fact, both samples exhibited inverse cubic spinel structure of Fe_3O_4 (JCPDS No. 85-1436). Notably, the observed XRD peaks are rather broad, which indicate the fine crystal size for the IONPs. By the Debye–Sherrer equation ($D=K\lambda/\beta\cos\theta$), the average crystallite sizes of the synthesized EDTA-Zn-SPIONs and PVC-Zn-SPIONs samples were calculated 7.1 nm and 8.2 nm, respectively.

3.2. FT-IR

To determine the surface coat onto the surface of the prepared iron oxide samples, FT-IR spectra were provided and presented in Fig. 2.

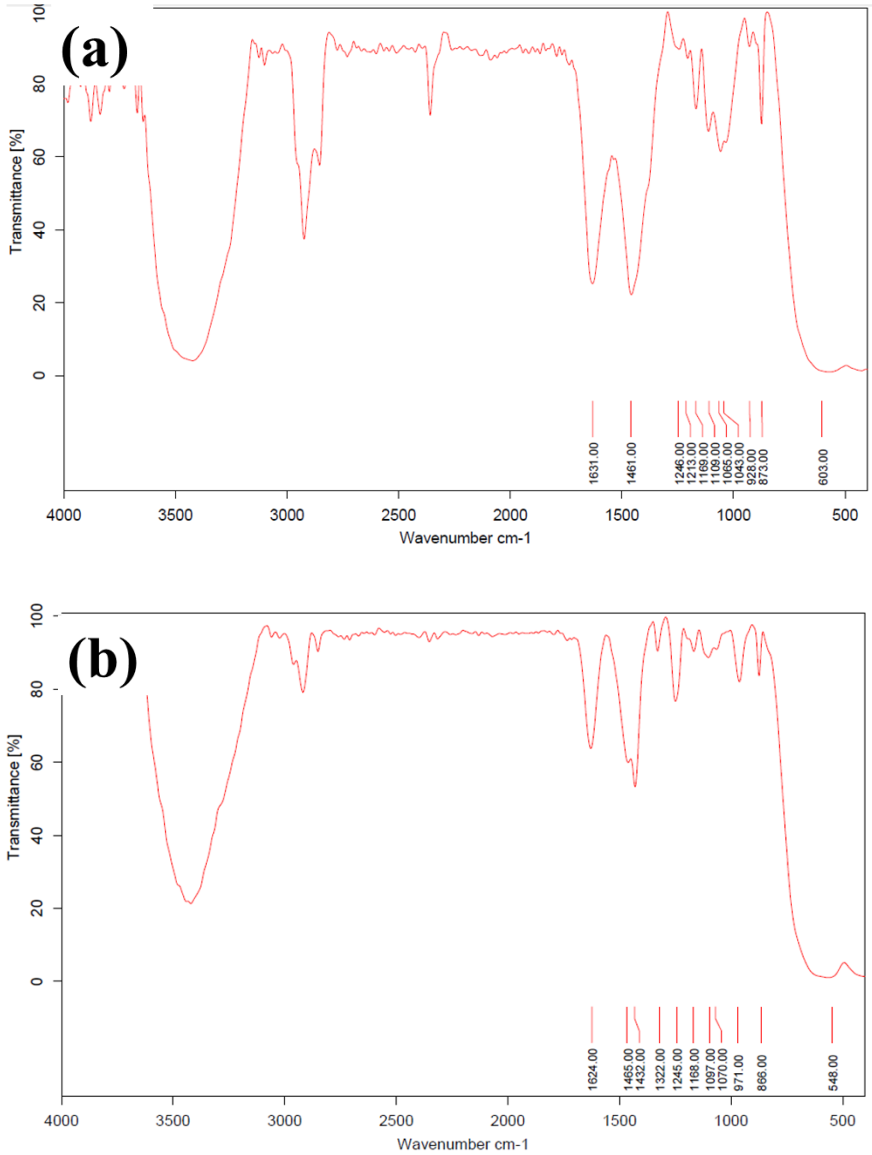

Fig. 2. IR spectra of the prepared (a) EDTA-Zn-SPIONs and (b) PVC-Zn-SPIONs

For the synthesized EDTA-Zn-SPIONs sample (Fig. 2a), the various IR bands are seen at the wavenumbers of 3450-3500 cm^{-1}, 3240 cm^{-1}, 2928 cm^{-1}, 2886 cm^{-1}, 2822 cm^{-1}, 1631 cm^{-1}, 1461 cm^{-1}, 1382 cm^{-1}, 1213 cm^{-1}, 1169 cm^{-1}, 1065 cm^{-1}, 1043 cm^{-1}, 928 cm^{-1}, 873 cm^{-1}, 603 cm^{-1} and 424 cm^{-1}. These IR absorptions are related to the different vibration modes of following of chemical bonds [33,61-68]; $\nu_{OH\ stretching}$ (at 3450-3500 cm^{-1}), $\nu_{C\text{-}C\ stretching}$ (at 928 cm^{-1}), $\nu_{C\text{-}N\ stretching}$ (at 1065 cm^{-1}), $\nu_{\text{-}CH2\ stretching}$ (at 1382 cm^{-1}), $\nu as_{CH2\ stretching}$ (at 2928 cm^{-1}), $\nu sy_{CH2\ stretching}$ (at 2886 cm^{-1}),$\nu_{\text{-}C\text{-}H\ stretching}$ (at 1169 cm^{-1}), $\nu_{COH\ stretching}$ (at 1461cm^{-1}), $\nu_{N\text{-}H\ stretching}$ (at 3240 cm^{-1}), $\nu_{\text{-}N\text{-}CH\ stretching}$ (at 2822 cm^{-1}), $\nu_{C\text{-}O\ scissoring}$ (at 1631 cm^{-1}), $\nu_{OH\ bending}$ (at 866 cm^{-1}), $\nu_{1(Fe\text{-}O\text{-}Fe\ stretching)}$ (at 603 cm^{-1}), $\nu_{1(Fe\text{-}O\text{-}Zn\ stretching)}$ (at 603 cm^{-1}), and $\nu_{2(Fe\text{-}O\text{-}Fe\ stretching)}$ (at 424 cm^{-1}). These IR bands confirmed that the prepared sample has composition of Zn-doped Fe_3O_4 and also EDTA on the particles surfaces.

For the electrodeposited PVC-Zn-SPIONs sample (Fig. 2b), there are the IR bands at the 3450-3500 cm^{-1}, 2936 cm^{-1}, 2874 cm^{-1}, 1624 cm^{-1}, 1465 cm^{-1}, 1432 cm^{-1}, 1322 cm^{-1}, 1168 cm^{-1}, 1097 cm^{-1}, 1070 cm^{-1}, 866 cm^{-1}, 548 cm^{-1} and 431 cm^{-1}. These IR peaks can be assigned to the following bond vibrations [66-70]; $\nu_{OH\ stretching}$ (at 3450-3500 cm^{-1}), $\nu as_{CH2\ stretching}$ (at 2936 cm^{-1}), $\nu sy_{CH2\ stretching}$ (at 2874 cm^{-1}), $\nu_{C\text{-}C\ bending}$ (at 1168 cm^{-1}), $\nu_{C\text{-}C\ stretching}$ (at 1070 cm^{-1}), $\nu_{C\text{-}Cl\ bending}$ (at 866 cm^{-1}), $\nu_{C\text{-}H\ scissoring}$ (at 1465 cm^{-1}), $\nu_{CH2\ deformations}$ (at 1322 cm^{-1}), $\nu_{\text{-}CH2\ stretching}$ (at 1432 cm^{-1}), $\nu_{CH\ bending}$ (at 1168 cm^{-1}), $\nu_{H2O\ stretching}$ (at 1624 cm^{-1}), $\nu_{CH2\ bending}$ (at 1097 cm^{-1}), $\nu_{1(Fe\text{-}O\text{-}Fe\ stretching)}$ (at 548 cm^{-1}), $\nu_{1(Fe\text{-}O\text{-}Zn\ stretching)}$ (at 548 cm^{-1}), and $\nu_{2(Fe\text{-}O\text{-}Fe\ stretching)}$ (at 431 cm^{-1}). The existence of these IR absorptions clearly proved the successful formation of PVC grafted Zn-doped SPIONs.

3.3. Surface morphology

FE-SEM observations, EDAX profiles and related elemental data for both prepared EDTA-Zn-SPIONs and PVC-Zn-SPIONs samples are provided and presented in Fig. 3. For these samples, the particle morphologies with uniform sized and complete spherical shape are seen in Figs. 3a and b. The average particle sizes for EDTA-Zn-SPIONs and PVC-Zn-SPIONs samples are measured to be 15nm and 20nm, respectively. These findings showed that the deposited iron oxide particles in the presence of EDTA have smaller size than those electro-synthesized in the presence of PVC agent. The EDAX profiles of EDTA-Zn-SPIONs and PVC-Zn-SPIONs samples are also given in Figs. 3c and d, respectively. In the composition of the EDTA-grafted EDTA-Zn-SPIONs sample, the elements of carbon, nitrogen, oxygen, iron and zinc are confirmed from the provided EDAX in Fig. 3c. The zinc presence revealed the metal cations doping into iron oxide during the electrochemical fabrication. Furthermore, the EDTA grafting onto the iron oxides surfaces is also indicated from EDAX measurement, where carbon and nitrogen element are observed in the EDAX profile presented in Fig. 3c. The weight percentages of carbon, nitrogen, oxygen, iron and zinc elements are also measured to be 15.5%, 2.01%, 37.37%, 36.33% and 8.97%,

respectively. From these data, it is revealed that the zinc doping into iron oxide crystal structure is about 8.79%wt. For the PVC-Zn-SPIONs sample, the same arguments for surface capping and metal-ion doping can be presented from EDAX profile and data from Fig. 3d.

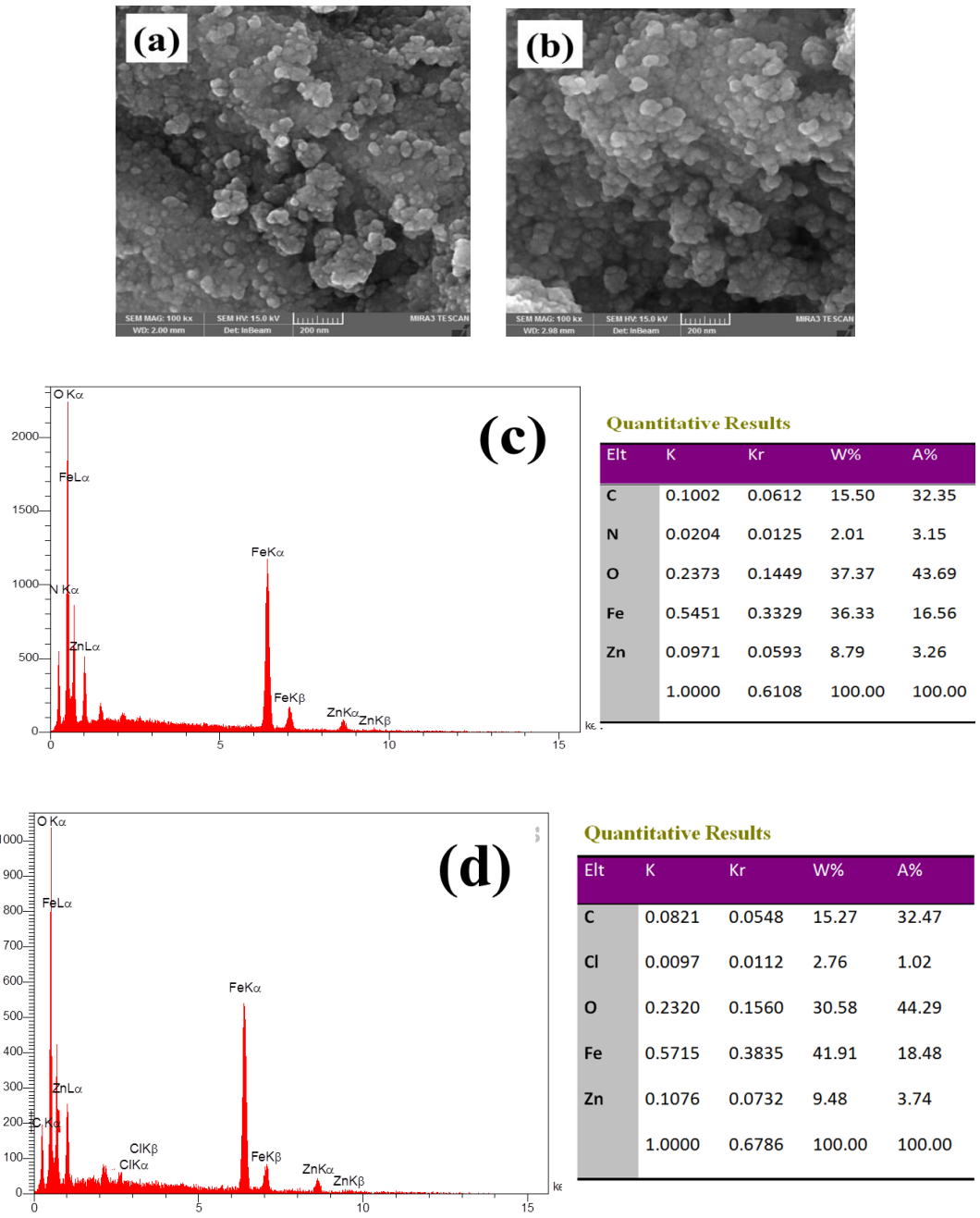

Quantitative Results

Elt	K	Kr	W%	A%
C	0.1002	0.0612	15.50	32.35
N	0.0204	0.0125	2.01	3.15
O	0.2373	0.1449	37.37	43.69
Fe	0.5451	0.3329	36.33	16.56
Zn	0.0971	0.0593	8.79	3.26
	1.0000	0.6108	100.00	100.00

Quantitative Results

Elt	K	Kr	W%	A%
C	0.0821	0.0548	15.27	32.47
Cl	0.0097	0.0112	2.76	1.02
O	0.2320	0.1560	30.58	44.29
Fe	0.5715	0.3835	41.91	18.48
Zn	0.1076	0.0732	9.48	3.74
	1.0000	0.6786	100.00	100.00

Fig. 3. FE-SEM images and EDAX curves and elemental data of the prepared (a,c) EDTA-Zn-SPIONs and (b,d) PVC-Zn-SPIONs samples

As seen in the EDAX profile in Fig. 3d, the elements of Cl, C, O, Fe and Zn are detected with weight percentages of 2.76%, 15.27%, 30.58%, 41.91% and 9.48%, respectively. The

zinc content in EDAX curve confirmed the doping of iron oxides of PVC-grafted IONPs with about 10% Zn cations. Also, the surface grafting with PVC polymer was also verified through chlorine element. In final, the FE-SEM observation and EDAX analysis clearly proved the facile preparation of EDTA- and PVC grafted iron oxide particles and also the zinc doping into Fe_3O_4 crystal structure.

3.4. Magnetic evaluation

The magnetic profiles of the EDTA-Zn-SPIONs and PVC-Zn-SPIONs samples are shown in Fig. 4. For both samples exhibited the superparamagnetic behavior. Saturation magnetization value of *Ms*=34.12 emu/g was measured for the EDTA-Zn-SPIONs, revealing the suitable magnetization performance of this sample at the presence of applied field. Also, the remanent (*Mr*) value of 0.29 emu/g was detected for this sample (as donated in Fig. 4a), which showed the good magnetic action at the absence of applied field. Furthermore, the EDTA-Zn-SPIONs sample exhibited the positive and negative remanent (i.e. $Mr_{(+)}$ and $Mr_{(-)}$) values of +0.21 emu/g and -0.38 emu/g, respectively (Fig. 4b). The coercivity for the EDTA-Zn-SPIONs can be also calculated from VSM curve at the low applied field (Fig. 4b) [69,70]. The EDTA-Zn-SPIONs sample showed coercivity (*Hci*) value of 9.1G, positive and negative coercivities of *Hci(+)*=11.28G and $Hci_{(-)}$=-6.75 G, indicating the optimal magnetic ability of this sample. The magnetic data of PVC-Zn-SPIONs sample is also provided in Fig. 4.

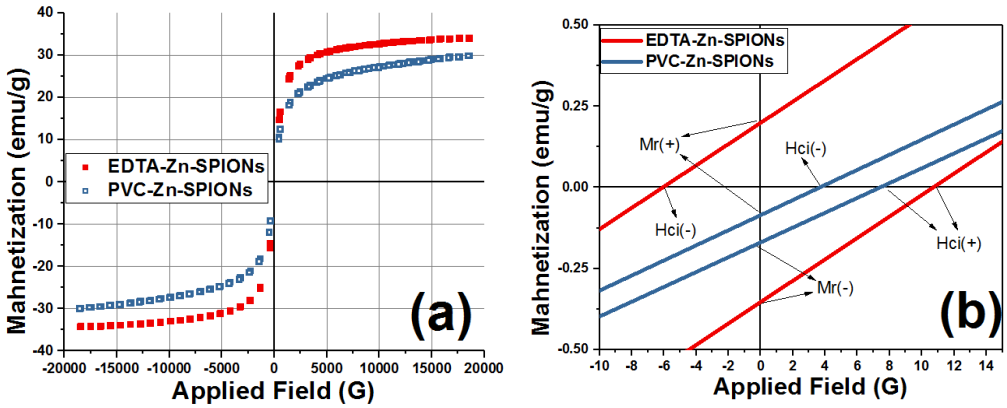

Fig. 4. Magnetization profiles of EDTA-Zn-SPIONs and PVC-Zn-SPIONs samples

This powder showed *Ms* and *Hci* values of 28.45 emu/g and 5.75 G, respectively, confirming the favorable magnetization capability of the PVC-grafted iron oxide nanoparticles. Furthermore, these nanoparticles exhibited remanent values of *Mr*=0.14 emu/g, $Mr_{(+)}$=-0.11 emu/g and $Mr_{(-)}$=-0.18 emu/g (as observable in Fig. 4b). These remanent data proved the good behavior of PVC coated Zn-SPIONs at the conditions of field removing. The positive and negative coercivity values of *Hci(+)*=7.75G and $Hci_{(-)}$=3.75 G (Fig. 4b) were observed at the absence of applied field for the PVC-Zn-SPIONs sample, proving the

superparamagnetic nature of this sample. In final, the quality of magnetic performances of both prepared samples was proved through VSM measurements, and hence these particles have optimal qualification for biomedical aims.

4. CONCLUSION

Reductive cathodic deposition was successfully used to obtain ethylenediaminetetraacetic acid- and polyvinyl chloride-grafted Zn^{2+}-doped iron oxide nanoparticles in a one-step procedure. The prepared particles have 15-20nm size and magnetite crystal structure. Furthermore, both PVC- and EDTA-grafted iron oxide powders exhibited superparamagnetic nature, where they showed *Hci*=5.75G and *Mr*=0.14 emu/g (for PVC-Zn-SPIONs) and *Mr*=0.29 emu/g and *Hci*= 9.1G (for EDTA-Zn-SPIONs).

REFERENCES

[1] G. Ciofani, "Smart Nanoparticles for Biomedicine" (2018) Elsevier, 1st Edition, ISBN: 9780128141564.

[2] F. Ahmadi, M. Rahimi-Nasrabadi, and M. Behpour, J. Mater. Sci.: Mater. Electron. 28 (2017) 1531.

[3] E. Kowsari, A. Ehsani, S. Assadi, and R. Safari, J. Electroanal. Chem. 826 (2018) 65.

[4] M. Rahimi-Nasrabadi, M. Rostami, F. Ahmadi, A.F. Shojaie, and M.D. Rafiee, J. Mater. Sci.: Mater. Electron. 27 (2016) 11940.

[5] K. Müller, E. Bugnicourt, M. Latorre, M. Jorda, Y. Echegoyen Sanz, J.M. Lagaron, Oliver Miesbauer, A. Bianchin, and S. Hankin, Nanomater. 7 (2017) 74.

[6] F.B. Ajdari, E. Kowsari, and A. Ehsani, J. Solid State Chem. 265 (2018) 155.

[7] J. Liu, S.Z. Qiao, Q.H. Hu, and G.Q. Lu, Small 7 (2011) 425.

[8] M. Rahimi-Nasrabadi, F. Ahmadi, and M. Eghbali-Arani, J. Mater. Sci.: Mater. Electron. 28 (2017) 2415.

[9] L. Fotouhi, N. Fathali, and A. Ehsani, Int. J. Hydrogen Energy 43 (2018) 6987.

[10] J. Sebastian Basuki, H.T.T. Duong, A. Macmillan, R. Whan, C. Boyer, and T.P. Davis, Macromol. 46 (2013) 7043.

[11] M. Barrow, A. Taylor, P. Murray, M.J. Rosseinsky, and D.J. Adams, Chem. Soc. Rev. 44 (2015) 6733.

[12] K. Turcheniuk, A.V. Tarasevych, V.P. Kukhar, R. Boukherroub, and S. Szunerits, Nanoscale 5 (2013) 10729.

[13] M. Aghazadeh, I. Karimzadeh, and M.R. Ganjali, Mater. Lett. 228 (2018) 137.

[14] M. Wang, G. Siddiqui, O.J. R. Gustafsson, A. Käkinen, I. Javed, N.H. Voelcker, D.J. Creek, P.C. Ke, and T.P. Davis, Small 13 (2017) 1701528.

[15] M. Aghazadeh, I. Karimzadeh, and M.R. Ganjali, J. Electronic Mater. 47 (2018) 3026.

[16] G. Hemery, E. Garanger, S. Lecommandoux, A.D. Wong, E.R. Gillies, B. Pedrono, T. Bayle, D. Jacob, and O. Sandre, J. Phys. D: Appl. Phys. 48 (2015) 494001.
[17] T. Blin, A. Kakinen, E.H. Pilkington, A. Ivask, F. Ding, J.F. Quinn, M.R. Whittaker, P.C. Ke, and T.P. Davis, Polym. Chem. 7 (2016) 1931.
[18] M. Singh, N. Sviridenkova, N. Timur, A. Savchenko, I. Shetinin, and A. Majouga, J. Cluster Sci. 27 (2016) 1383.
[19] I. Karimzadeh, H. Rezagolipour Dizaji, and M. Aghazadeh, Mater. Res. Express. 3 (2016) 095022.
[20] I. Karimzadeh, H.R. Dizaji, and M. Aghazadeh, J. Magn. Magn. Mater. 416 (2016) 81.
[21] Y. Wang, F. Wang, Y. Shen, Q. He, and S. Guo, Mater. Horiz. 5 (2018) 184.
[22] W. Wu, C. Zhong Jiang, and V.A.L. Roy, Nanoscale 8 (2016) 19421.
[23] M. Aghazadeh, and I. Karimzadeh, Curr. Nanosci. 14 (2018) 42.
[24] D.C. Manatunga, R.M. de Silva, K.M. Nalinde Silva, N. Silva, S. Bhandari, Y.K. Yap, and N.P. Costha Europ. J. Pharm. Biopharm. 117 (2017) 29.
[25] X. Zhou, Q. Zhang, L. Chen, W. Nie, W. Wang, H. Wang, X. Mo , and C. He, ACS Biomater. Sci. Eng. 5 (2019) 710.
[26] M. Aghazadeh, I. Karimzadeh, M.R. Ganjali, and M. Mohebi Morad, Mater. Lett. 196 (2017) 392.
[27] I. Karimzadeh, M. Aghazadeh, M.R. Ganjali, P. Norouzi, T. Doroudi, and P.H. Kolivand, Mater. Lett. 189 (2017) 290.
[28] I. Karimzadeh, M. Aghazadeh, M.R. Ganjali, P. Norouzi, S. Shirvani-Arani, T. Doroudi, P.H. kolivand, S. A. Marashi, and D. Gharailou, Mater. Lett. 179 (2016) 5.
[29] F. Liu, C. Shan, X. Zhang, Y. Zhang, W. Zhang, and B. Pan, J. Hazardous Mater. 321 (2017) 290.
[30] D. Zhao, Q. Zhang, H. Xuan, Y. Chen, K. Zhang, S. Feng, A. Alsaedi, T. Hayat, and C. Chen, J. Colloid Interface Sci. 506 (2017) 300.
[31] Y. Liu, R. Fu, Y. Sun, X. Zhou, S.A. Baig, and X. Xu, Appl. Surf. Sci. 369 (2016) 267.
[32] Y. Ren, H.A. Abbood, F. He, H. Peng, and K. Huang, Chem. Engin. J. 226 (2013) 300.
[33] A.G. Magdalena, I.M.B. Silva, R.F.C. Marques, A.R.F. Pipi, P.N. Lisboa-Filho, and M. Jafelicci, J. Phys. Chem. Solids 113, (2018) 5.
[34] E. Repo, J.K. Warcholc, T.A. Kurniawana, and M.E.T. Sillanpää, Chem. Engin. J. 161 (2010) 73.
[35] E. Ghasemi, A. Heydari, and M. Sillanpää, Microchem. J. 131 (2017) 51.
[36] L. Cui, Y. Wang, L. Gao, L. Hu, L. Yan, Q. Wei, and B. Du, Chem. Engin. J. 281 (2015) 1.
[37] M. Aghazadeh, M.G. Maragheh, M.R. Ganjali, and P. Norouzi, RSC Adv. 6 (2016) 10442.
[38] M. Aghazadeh, and M.R. Ganjali, J. Mater. Sci.: Mater Electron. 28 (2017) 11406.

[39] M. Aghazadeh, and M.R. Ganjali, J. Mater. Sci.: Mater Electron. 28 (2017) 8144.
[40] M. Aghazadeh, J. Mater. Sci.: Mater. Electron. 28 (2016) 3108.
[41] M. Aghazadeh, A.A.M. Barmi, and M. Hosseinifard, Mater. Lett. 73 (2012) 28.
[42] M. Aghazadeh, M.G. Maragheh, M.R. Ganjali, and P. Norouzi, Inorg. Nano-Metal Chem. 27 (2017) 1085.
[43] M. Aghazadeh, M.R. Ganjali, and P. Norouzi, Mater. Res. Express 3 (2016) 055013.
[44] M. Aghazadeh, and M.R. Ganjali, J. Mater. Sci. 53 (2018) 295.
[45] M. Aghazadeh, A.A.M. Barmi, H.M. Shiri, and S. Sedaghat, Ceram. Int. 39 (2013) 1045.
[46] M. Aghazadeh, J. Mater. Sci.: Mater. Electron. 28 (2017) 18755.
[47] M. Aghazadeh, M. Ghaemi, A.N. Golikand, and A. Ahmadi, Mater. Lett. 65 (2011) 2545.
[48] M. Aghazadeh, I. Karimzadeh, and M.R. Ganjali, J. Mater. Sci.: Mater. Electron. 28 (2017) 13532.
[49] N. Sanpo, C.C. Berndt, C. Wen, and J. Wang, Handbook Nanoelectrochem. (2015) doi: 10.1007/978-3-319-15207-3-12-1.
[50] W. Xiao, X. Zeng, H. Lin, K. Han, H.Z. Jia, and X.Z. Zhang, Chem. Commun. 51 (2015) 1475.
[51] E. Shah, P. Upadhyay, M. Singh, M.S. Mansuri, R. Begum, N. Shethd, and H. P. Soni, New J. Chem. 40 (2016) 9507.
[52] M.H. Hsiao, Q. Mu, Z.R. Stephen, C. Fang, and M. Zhang, ACS Macro Lett. 4 (2015) 403.
[53] M. Aghazadeh, and M.R. Ganjali, J. Mater. Sci.: Mater. Electron. 29 (2018) 2291.
[54] M. Aghazadeh, and M.R. Ganjali, J. Mater. Sci.: Mater. Electron. 29 (2018) 4981.
[55] M. Aghazadeh, I. Karimzadeh, M. Ghannadi Maragheh, and M.R. Ganjali, Korean J. Chem. Engin. 35 (2018) 1341.
[56] M. Aghazadeh, I. Karimzadeh, and M.R. Ganjali, Mater. Res. 21 (2018) e20180094.
[57] M. Aghazadeh, I. Karimzadeh, and M.R. Ganjali, J. Mater. Sci.: Mater. Electron. 28 (2017) 19061.
[58] M. Aghazadeh, I. Karimzadeh, M.R. Ganjali, and A. Behzad, J. Mater. Sci.: Mater. Electron. 28 (2017) 18121.
[59] M. Aghazadeh, I. Karimzadeh, and M.R. Ganjali, J. Mater. Sci.: Mater. Electron. 29 (2018) 5163.
[60] M. Aghazadeh, and I. Karimzadeh, Mater. Res. Express 4 (2017) 105505.
[61] C.L. Warner, R.S. Addleman, and A.D. Cinson, Chem. Sus. Chem. 3 (2010) 749.
[62] Y. Huang, and A.A. Keller, Water Res. 80 (2015) 159.
[63] M. Aghazadeh, Mater. Lett. 211 (2018) 225.
[64] M. Aghazadeh, and M.R. Ganjali, Ceram. Int. 44 (2018) 520.

[65] L. Yang, Y. Li, L. Wang, Y. Zhang, X. Ma, and Z. Ye, J. Hazardous Mater. 180 (2010) 98.

[66] K. Yao, J. Gong, N. Tian, Y. Lin, X. Wen, Z. Jiang, H. Na, and T. Tang, RSC Adv. 5 (2015) 31910.

[67] F. Reyes-Ortega, A.V. Delgado, E.K. Schneider, B.L.C. Fernande, and G.R. Iglesias, Polymers 10 (2018) 10.

[68] M. Aghazadeh, I. Karimzadeh, and M. R. Ganjali, Curr. Nanosci. 15 (2019) 169.

[69] C. Barrera, A. P. Herrera, N. Bezares, E. Fachini, R. Olayo-Valles, J. P. Hinestroza, and C. Rinaldi, J. Colloid Interface Sci. 377 (2012) 40.

[70] M. Aghazadeh, and K. Yavari, Anal. Bioanal. Electrochem. 10 (2018) 1426.